Contents lists available at ScienceDirect

Chemical Engineering Research and Design

journal homepage: www.elsevier.com/locate/cherd

Effect of particle contact point treatment on the CFD simulation of the heat transfer in packed beds

Mario Pichler[a], *Bahram Haddadi*[a,*], *Christian Jordan*[a], *Hamidreza Norouzi*[b], *Michael Harasek*[a]

[a] *Institute of Chemical, Environmental & Bioscience Engineering, TU Wien, Getreidemarkt 9/166, 1060 Vienna, Austria*

[b] *Department of Chemical Engineering, Amirkabir University of Technology, Tehran, Iran*

ARTICLE INFO

Article history:
Received 16 June 2020
Received in revised form 30 October 2020
Accepted 2 November 2020
Available online 12 November 2020

Keywords:
Packed bed
Heat transfer
Contact point modification
Design of simulation experiments

ABSTRACT

In recent years, computational fluid dynamic (CFD) simulation of fully resolved fixed beds has become a popular tool for getting deeper insight in local phenomena in packed beds. To get correct simulation results, special care has to be taken on how to treat particle/particle and particle/wall contact points.

In this work a local contact point modification, the local bridges method is investigated to study its effect on the heat transfer in packed beds. Packings were created using the Discrete Element Method (DEM) software discrete Flow, and were modified to implement the bridges. Using Design of Simulation Experiments (DoSE) the influence of different parameters on the heat transfer was studied. The simulated heat transfer in packed beds, considering conduction as well as natural convection, is compared to measurements and well-established correlations. Based on the Design of Simulation Experiments, a model for the correction of the effective thermal conductivity of bridges, to reduce the simulation error as a function of particle diameter D, is suggested. The suggested correction was tested on spheres of different material and sizes to check its validity. Using this correction, the simulation error for the beds surface temperature could be reduced by 75 % in a representative example case.

© 2020 Institution of Chemical Engineers. Published by Elsevier B.V. All rights reserved.

1. Introduction

In chemical process industry, fixed-bed units are used for many chemical unit operations, e. g. in separation processes, absorption, adsorption and also commonly in catalytic reactors. Coupled partial differential equations that describe momentum, energy and material balances together with equilibrium equations and transport rates, are required for a full mathematical description of fixed-bed columns. Due to the complexity of solving such coupled stiff partial differential equation systems, simplifications are made, to reduce the effort of solving the problem. Consequently, many different models exist, that are only valid for certain operating conditions under particular situations (VDI-Wärmeatlas, 2013; Shafeeyan et al., 2014).

However, the conventional plug flow based or pseudo-continuum models do not consider actual structure of the fixed bed and therefore phenomena caused by local concentrations and temperatures (Channelling, local backflow or stagnation, radial heat transfer or local kinetics). For catalytic reactions and adsorption processes, local phenomena, e. g. local temperature peaks, are one of the most important factors for the correct description of the process (Dixon and Nijemeisland, 2001). These local effects can be described by simulation of fully resolved fixed bed columns using computational fluid dynamics (CFD). However, there are some

* Corresponding author.
E-mail addresses: mario.pichler@tuwien.ac.at (M. Pichler), bahram.haddadi.sisakht@tuwien.ac.at (B. Haddadi), christian.jordan@tuwien.ac.at (C. Jordan), h.norouzi@aut.ac.ir (H. Norouzi), michael.harasek@tuwien.ac.at (M. Harasek).
https://doi.org/10.1016/j.cherd.2020.11.005
0263-8762/© 2020 Institution of Chemical Engineers. Published by Elsevier B.V. All rights reserved.

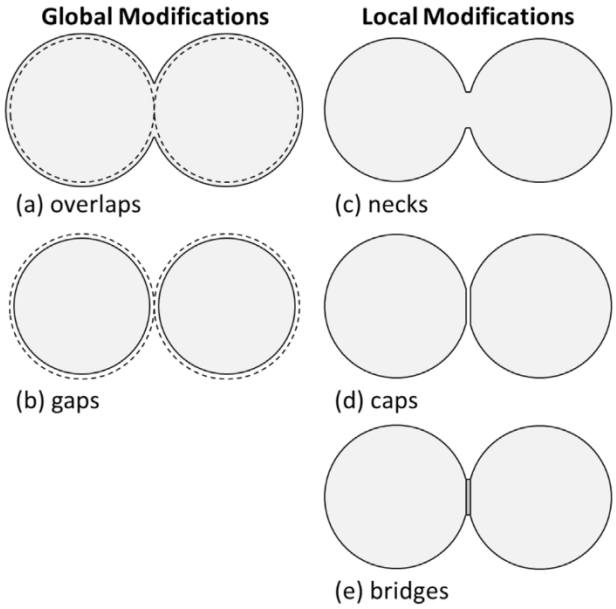

Fig. 1 – Different global and local contact point modification methods. The grey area represents to adjacent spheres after the contact point treatment.
a) overlaps: increasing the original particle diameter (dashed lines) to create overlapping spheres
b) gaps: decreasing the original particle diameter (dashed lines) to create a gap between spheres
c) necks: introducing a cylinder at contact points, which is treated as part of the spheres.
d) caps: introducing a cylinder at contact points, which is treated as fluid.
e) bridges: introducing a cylinder at contact points, which is treated as a separate region. An effective thermal conductivity is assigned to this region.

difficulties in discretizing (meshing) an actual packed bed, due to complexity of the packing and particle/particle and particle/wall contacts. Automatic meshing of the bed geometry can lead to extremely skewed cells around contact points, which can result in unstable simulations. Many authors have studied different contact-point modifications, in order to improve solution stability by avoiding low quality meshing and to ensure correct prediction of pressure drop and heat transfer in the packed beds (e.g. Dixon and Nijemeisland, 2001; Kuroki et al., 2007; Yang et al., 2012; Wehinger, 2016).

There are different ways to deal with contact points in packed beds. Global packing modifications try to avoid the contact point problem by increasing or decreasing the particle diameter. This leads to an overlap or gap between individual particles, respectively. However, when using global modifications, the bed porosity is changed drastically. Local contact point treatments (necks, caps, bridges) have less influence on the bed porosity, thus is preferable to global methods. Widely used global and local modifications are shown in Fig. 1. All these methods and their influence on heat transfer and pressure drop have been studied by several authors, as discussed below.

To avoid contact points, many authors used global methods to treat contact points. Two global modification methods ate the so-called overlaps method (Fig. 1a) and the gaps method (Fig. 1b) (Dixon et al., 2011). Here the particle diameter is increased or decreased to get overlapping particles or gaps between particles respectively.

Dixon and Nijemeisland (2001) used the gaps method with different scaling factors to simulate not only the velocity field, but also wall to fluid heat transfer for 44-spheres and a particle diameter to bed diameter ratio of $N = D_{col}/D = 2$. Guardo et al. (2004), who expanded the spheres by 1 % of their diameter. Simulations have been carried out using particle Reynolds numbers Re_p of up to 912 and bed diameter to particle used the opposite approach, the overlaps method. Here the simulated pressure drop along the bed is slightly higher compared to the Ergun equation (Ergun, 1952), but shows good agreement for particle Reynolds numbers of up to 1000. Other authors as well applied the overlaps method to avoid the contact point problem (e.g. Behnam et al., 2013). However, global modifications have big impact on the overall packing structure, more precisely the porosity. A change in diameter of 1 % results in up to 10–15% deviation of the drag coefficient (Dixon et al., 2013).

A different approach was introduced by Ookawara et al. (2007) and Kuroki et al. (2007). They used the necks (Fig. 1c) method to calculate the pressure drop and wall to fluid heat transfer in packed beds. The authors linked particles by placing cylinders with different diameter in between adjacent spheres. The interior of the spheres was not part of the computational domain. The counterpart of the necks method, the so-called caps method (Fig. 1d) was used by Eppinger et al. (2011). The authors moved the vertices at close proximity of contact points towards particle centres to get small caps between particles, to simulate the pressure drop along the bed.

Only few authors compared the influence of different methods to treat contact points on the pressure drop, temperature and velocity fields. Dixon et al. (2013) tested the different local and global contact point modification methods for spherical particles. In their study, the bridges method (Fig. 1e) was introduced. In contrary to the necks method, where the cylinders are treated as part of the packing with same thermal properties, bridges are treated as separate regions. This allows assigning thermal properties, which are different from the packing properties. They concluded that global methods lead to unacceptable high errors in pressure drop and heat transfer. The authors recommended using caps or bridges with a bridge to particle diameter ratio $d/D \leq 0.2$ in order to get a reasonable pressure drop. For the simulation of heat transfer at particle Reynolds numbers $Re_p \leq 2000$, bridges with $d/D \leq 0.2$ can be used. For $Re_p \geq 2000$ the bridge size should be restricted to $d/D \leq 0.1$. In all cases, an effective thermal conductivity should be assigned to the bridges.

Bu et al. (2014) studied the influence of gaps, overlaps, bridges and caps as contact point treatment on the pressure drop and heat transfer in structured beds and compared the simulated results to experiments carried out by Yang et al. (2012). They found that gaps and overlaps lead to remarkable changes in porosity and therefore in pressure drop and are therefore not suitable for pressure drop simulations. The authors concluded that bridges with $d/D = 0.16$ up to $d/D = 0.2$ should be used in structured packed beds.

Wehinger (2016) showed that the difference in porosity for the caps and the bridges method used for cylindrical particles is less than 1 % (absolute). The pressure drop changed by approximately 15 % from the lowest value, using caps, to the highest value, using bridges. Different contact point treatments, including bridges, necks and caps, have been used to simulate the heat transfer for cylindrical particles. Necks at heater-particle contacts, with the same conductivity as the particles, gave the highest temperatures. Bridges with dif-

ferent conductivities and the local caps method gave close results. The author concluded that for high Reynolds numbers the influence of the contact-point treatment is getting less important for radial heat transfer, as convective heat transfer is dominant. Furthermore, they pointed out that the thermal conductivity of the bridges can be used as a tuning parameter to get correct heat transfer.

Bu et al. (2020) showed that at low temperatures (<400 K) the contact point conduction is the dominating heat transfer component in packings with stagnant fluid. They also showed that the share of radiation increases with increasing temperatures. For high solid to fluid thermal conductivity ratios, the solid to fluid conduction has low influence on the overall heat transfer.

Cheng et al. (2020) calculate the effective thermal conductivity of packed beds, considering the bed structure based on Voronoi–Delaunay tessellation. They showed that conduction through voids in between particles can be neglected for high ratios of solid to fluid conductivity ratios (>5).

However, the focus of most of these works has been columns with forced fluid flow, mostly radial heat transfer and particles with low thermal conductivities. There, the dominant heat transfer mechanism is convection and radiation, and the contribution of conductive heat transfer is small. In the present work the bridges contact point treatment method has been studied. This method was chosen, due to its flexibility. The conductivity in the bridges can be modified and used as a tuning parameter. Experiments and simulations of packings with up to 619 particles and particle diameters of D = 6–10 mm were performed. The influence of the particle diameter, bridge sizes and effective thermal conductivities in the bridges on the heat transfer is investigated using Design of Simulation Experiments (DoSE). A correction factor for the effective thermal conductivity of bridges, accounting for non-ideal contact points due to flattening, surface roughness and non-spherical particles, is presented and validated.

2. Experimental setup

Using different sized spherical particles, a set of experiments was performed to study heat transfer caused by natural convection and conduction in the packed beds. No forced convection is applied, to reduce the influence of convection on the heat transfer.

The experimental setup consists of an insulated rectangular container and an aluminium plate, on which the packing is placed. The packing is heated from bottom using two PTC (positive thermal coefficient of resistance) heaters mounted on the aluminium plate, with a total nominal power of 40 W and a maximal temperature of ~70 °C. The different parts and dimensions of the experimental setup can be seen in Fig. 2.

The surface temperature of the packed bed was measured with a platinum resistance sensor (Pt1000, Ø1.5 mm, precision within ± 0.2 K). To ensure close contact and accurate measurement of the packing's surface temperature, the platinum resistance sensor was soldered to a single sphere. This sphere was placed at the surface layer of the packing. To get not only the surface temperature of the packing at a single point, but also the temperature distribution a FLIR® E6 (FLIR® Systems, Inc; Wilsonville, Oregon) infrared camera was used (precision within ± 2 K). The top layer of spheres was painted black using matt high temperature paint to achieve a uniform emissivity. In addition, the heaters temperatures were measured in each experiment using platinum resistance sensor (Pt1000). This time dependent temperature profile was then used as a boundary condition in CFD simulation.

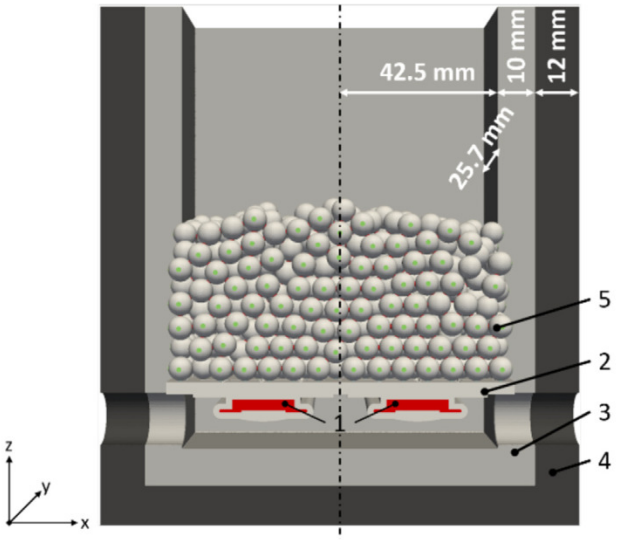

Fig. 2 – Cut view of experimental setup: 1: heating elements, 2: aluminium bottom plate (thickness 3 mm), 3: container, 4: insulation, 5: packing of spheres (maximum possible height: 98 mm).

Two types of materials were used for investigations: aluminium for the Design of Simulation Experiments and steel for validation. Material properties of the setup, the surrounding gas (air) and used packing material are shown in Table 1. All experiments were carried out at ambient pressure.

3. Packing creation, meshing and thermal properties of bridges

3.1. *Packing creation and meshing*

The method of choice to create packings was the Discrete Element Method (DEM). DEM is an extension of the Lagrangian modelling approach, in which inter-particular contact forces are included into the equation of motion. For calculating the contact forces, the soft particle formulation was used. In the soft-particle formulation, the contact forces, obtained from particle overlaps, are proportional to the overlap, the particle material and the geometric properties (Wehinger, 2016; Norouzi et al., 2016).

The discrete Flow DEM-software (in-house) was used to create the random packings. The open-source software SALMOE (version 8.4.0) was used for contact point treatment and to create and export the surface mesh of packing and bridges.

The bed creation and simulation procedure is shown in Fig. 3:

1 A defined number of particles is randomly created at an insertion plane and then injected with a given initial velocity
2 All particles are allowed to settle in stable position to create the final packing. No shaking or vibrating was carried out in this study to maintain the original porosity
3 The packing is imported into the geometry module (GEOM) of SALOME
4 Bridges are created with given bridge to particle diameter ratio d/D at contact-points

Table 1 – Properties of setup, air and particles.

Part	Property	Unit	Value	Reference
	Prandtl number Pr	–	0.7	
Fluid (air)	Heat capacity $c_{p,g}$	J/(kg K)	1004.5	
	Dynamic viscosity μ	Pa s	1.8×10^{-5}	
	Density ρ	Kg/m^3	1000	
Container	Heat capacity c_p	J/(kg K)	2050	
	Thermal conductivity k_s	W/(m K)	0.38	
	Density ρ	Kg/m^3	2700	
Bottom plate	Heat capacity c_p	J/(kg K)	837	
	Thermal conductivity k_s	W/(m K)	236	VDI-Wärmeatlas (2013)
	Density ρ	Kg/m^3	200	
Outside Insulation	Heat capacity c_p	J/(kg K)	2000	
	Thermal conductivity k_s	W/(m K)	0.03	
	Density ρ	kg/m^3	2700	
Aluminium	Heat capacity $c_{p,s}$	J/(kg K)	837	
	Thermal conductivity k_p	W/(m K)	236	
	Density ρ	kg/m^3	7850	
Carbon Steel	Heat capacity $c_{p,s}$	J/(kg K)	430	
	Thermal conductivity k_p	W/(m K)	54	

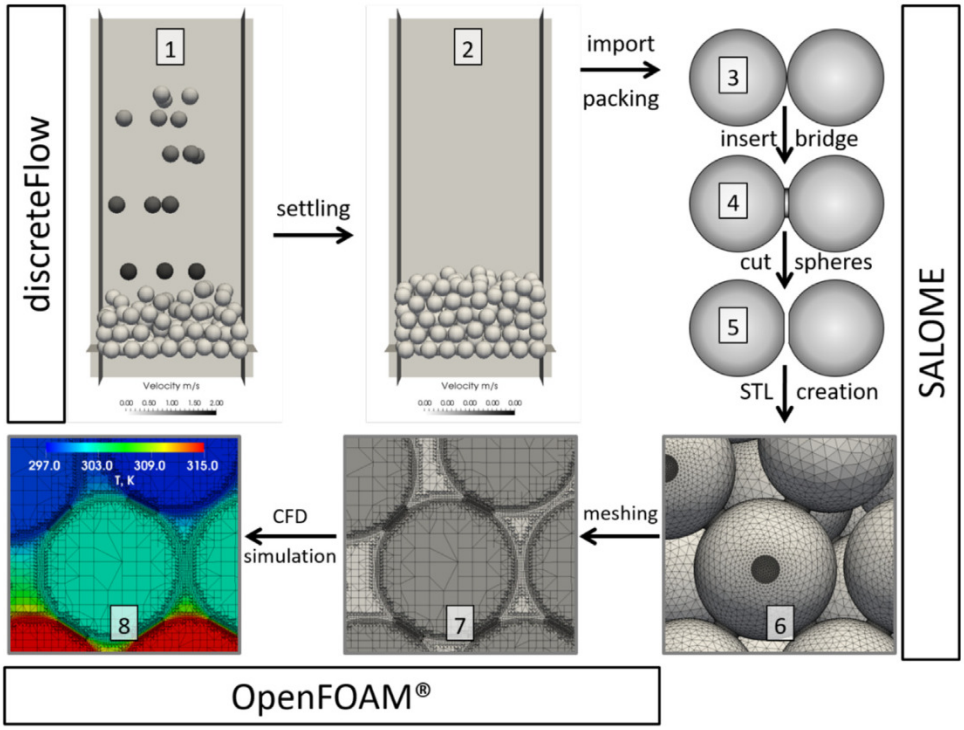

Fig. 3 – Procedure of creating a randomly packed bed of spheres. Bridges are inserted using SALOME before exporting the STL-files, which are then used for meshing.

5 Bridges are subtracted from the packing to get capped spheres
6 Surface mesh of packing and bridges is created using SALOME's mesh module (SMESH) and exported as STL-file
7 Using the surface representation of the packing, bridges and the setup, the mesh is created in the automated mesh generation tool snappyHexMesh
8 CFD Simulation of heat transfer using OpenFOAM

In step three bridges are only inserted at contact points, if the distance between particle surfaces or the distance between particle surface and wall is below a given value. In this study a threshold value of 1 % of the particle diameter was used.

For meshing in the automated mesh generation tool snappyHexMesh is used.

For the combination D =6 mm particles and d/D = 0.15 bridges only a quarter of the geometry is simulated, to get reasonable cell count. Thus symmetry boundary conditions have been used at cut planes in the CFD simulation. The number of cells for different cases was between 20 and 50 million cells.

3.2. *Thermal properties of bridges*

According to Dixon et al. (2013) it is obligatory to insert cylindrical bridges at contact points, to get reasonable results for heat transfer and pressure drop in packed beds. An effective thermal conductivity k_{eff} and particles heat capacity and density are assigned to the bridges.

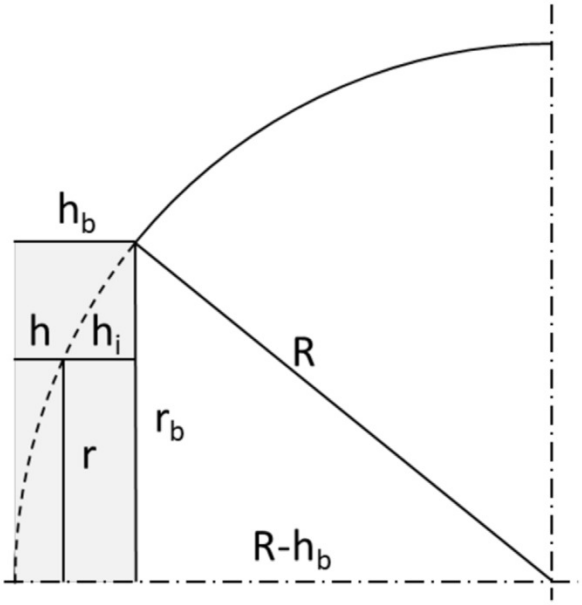

Fig. 4 – Geometry of the bridge and definition of the variables used in Equations (2013) – (5).

The effective thermal conductivity of the cylindrical bridges can be calculated using

$$k_{eff} = \frac{2h_b}{r_b^2}\int_0^{r_b} \frac{k_p k_{fr}}{h_i k_{fr} + h k_p} r dr \tag{1}$$

$$h_b = R - \sqrt{R^2 - r_b^2} \tag{2}$$

$$h = R - \sqrt{R^2 - r^2} \tag{3}$$

$$h_i = h_b - h \tag{4}$$

$$k_{fr} = \frac{k_f}{1 + \left(\frac{2\Lambda}{h}\right)(2-\gamma)/\gamma} \tag{5}$$

Geometrical variables are defined in Fig. 4. R is the particle diameter, r_b is the bridge radius, h_b is half the height of the bridge, h and h_i are half of the fluid conduction length between particles and half of the solid particle conduction length at a given radial position $0 \le r \le R$ between particles, k_p is the thermal conductivity of the particles, k_f is the thermal conductivity of the surrounding gas, k_{fr} is the reduced thermal conductivity of a gas-filled gap, γ is the accommodation coefficient and Λ is the mean free path of the gas molecules (Dixon et al., 2013).

Eq. (5) takes into account that the thermal conductivity in a gap needs to tend to zero as the gap width tends to zero, known as the Smoluchowski effect (Dixon et al. (2013). γ and Λ are calculated according to Eqs. (6 and 7) respectively.

$$\log\left(\frac{1}{\gamma} - 1\right) = 0.6 - \frac{1000/T + 1}{C} \tag{6}$$

$$\Lambda = 2\frac{2-\gamma}{\gamma}\sqrt{\frac{2\pi\mathcal{R}T}{M}}\frac{\lambda_f}{p\left(2c_{p,g} - \mathcal{R}/M\right)} \tag{7}$$

Here T is the gas temperature in Kelvin, λ_f is the fluid thermal conductivity, $c_{p,g}$ is the gas heat capacity, M is molar mass of the gas, $\mathcal{R}$ is the universal gas constant and the quantity C depends on molar mass of the gas (e.g. air: C = 2.8, VDI-Wärmeatlas, 2013).

The calculation of the effective thermal conductivity of the bridges at the contact point of two spheres is calculated under the following assumptions:

The thermal resistance at a given radius $0 \le r \le r_b$ can be described as two thermal resistances in series, namely the conduction through the particle ($0 \le h_i(r) \le h_b$, κ_p) and the conduction through the air in the gap ($0 \le h(r) \le h_b$, κ_f). Here h and κ are the conduction length end conductivity respectively.

- The particles are perfect spheres. Thus, h_b and h_i can be described using Eqs. (2–4)
- When analyzing Eqs. (2–4), it can be easily seen that the conduction length hi in the particle reaches $h_i = 0$ at exactly $r = r_b$ and $h_i = h_b$ at exactly r = 0. On the contrary the conduction length h in the fluid filled gap is h = 0 at r = 0 and $h_i = h_b$ at $r = r_b$. From that, it directly follows that a perfect contact point between particles is assumed.

Due to flattening (plastic and/or elastic deformation), surface roughness und non-ideal particle shape (non-spherical), the assumption of point contact is not fulfilled in real world applications. The contact point shifts to a contact area. Because of these imperfections, the calculated effective thermal conductivity of the bridges needs to be corrected. In the present study this is done using Design of Simulation Experiments.

3.3. Porosity

One of the most important global parameters contributing to the effective thermal conductivity of a packed bed is the porosity. To validate the DEM-created packing, the packing's porosity was compared to two commonly used equations.

The model of deKlerk (Norouzi et al., 2016) is given in Eqs. (8 and 9). Model equations proposed by deKlerk (2003) are given in Eqs. (10–12).

$$z \le 0.637 : \psi(r_{col}) = 2.14z^2 - 2.53z + 1 \tag{8a}$$

$$z > 0.637 : \psi(r_{col}) = \psi_\infty + 0.29e^{-0.6z}(\cos(2.3\pi(z - 0.16)) + 0.15e^{-0.9z} \tag{8b}$$

with

$$z = \frac{R_{col} - r_{col}}{D} \tag{9}$$

$$r^* < 0 : \psi(r_{col}) = \psi_{min} + (1 - \psi_{min})\, r_*^2 \tag{10a}$$

$$r^* \ge 0 : \psi(r_{col}) = \psi_\infty + (\psi_{min} - \psi_\infty)\, exp\left(-\frac{r^*}{a_1}\right) cos\left(\frac{\pi r^*}{b_1}\right) \tag{10b}$$

with

$$r^* = \left(\frac{R_{col} - r_{col}}{x_{min}}\right) - 1 \tag{11}$$

$$x_{min} = \frac{1}{2}D\left(\frac{D_{col}}{D} - \sqrt{\left(\frac{D_{col}}{D} - 1\right)^2 - 1}\right) \tag{12}$$

and the model constants $\psi_{min} = 0.24$, $a_1 = 4$, $b_1 = 0.876$. ψ_∞ in Eq. (8b) and Eq. (10a) is the porosity of an infinitely extended bed.

The porosity profile $\psi(r_{col})$ and average porosity ψ according to the models mentioned above were compared to the DEM-created sphere packing for different bridge sizes. The average porosities of a sphere packing with sphere diameter of D = 10 mm were ψ = 0.4423, ψ = 0.4418 for the DEM-created packing with d/D = 0.15 bridges and d/D = 0.2 bridges respectively. For Eqs. (8 ad 9) and Eqs. (10–12), and average porosities were ψ = 0.443 and ψ = 0.415, respectively. Apparently, the bridge size has very little influence on the packing porosity. When changing the bridge size from d/D = 0.15 to 0.2, the average porosity of the packing changes by 0.05 %. Both, the packings porosity profile and the average porosity, do match the calculated. Thus the packing creation method is considered to be valid.

To ensure similar porosities in simulation and experiments, the exact same number of spheres (619 spheres for D =6 mm and 200 spheres D = 10 mm) and the same filling height were used.

4. CFD simulations

Fluid flow and heat transfer in the solid and fluid can be described by following coupled partial differential equations:

$$\frac{\partial \rho}{\partial t} + \nabla.(\rho u) = 0 \tag{13}$$

$$\frac{\partial \rho u}{\partial t} + \nabla.\rho uu = -\nabla p + \nabla.\mu\left(\nabla u + \nabla^T u\right) \tag{14}$$

$$\frac{\partial \rho C_P T}{\partial t} + \nabla.\rho c_P T u = \nabla.k\left(\nabla T\right) + S_e \tag{15}$$

Eqs. (13)–(15) are the mass conservation (continuity) equation, the momentum conservation (Navier-Stokes) equations and the energy conservation equation, respectively. The finite volume method uses the integral form of the conservation equations as its starting point for solving these equations numerically. The solution domain is divided into a finite number of control volumes (CVs). The total of all CVs is called the grid or mesh. The conservation equations are applied to each CV. Interpolation is used to express variable values at CV surfaces in terms of the nodal values. The finite volume method can be used at any type of grid, so it is suitable for complex geometries (Bey and Eigenberger, 1997).

In this study, the open source software OpenFOAM® (version 4.1) and the standard OpenFOAM® solver *chtMultiRegionFoam* is used for the numerical solution of Eqs. 13–16. *chtMultiRegionFoam* is a solver which can simulate heat transfer in fluid and solid regions, including the heat transfer between them using mapped boundary conditions. The solver can also handle buoyancy flows considering the gravity and temperature dependent density. The relation between pressure p, temperature T and density ρ for the air in the gaps, is described using ideal gas equation

$$\rho = \frac{1}{\mathcal{R}T}p \tag{16}$$

where $\mathcal{R}$ is the specific gas constant.

Heat transfer between mesh zones was realized using mapped boundary conditions. No heat flux was allowed from the insulation to the surroundings. Air in- and outflow due to natural convection was allowed using a zero gradient boundary condition. The heaters temperature (parts (1) in Fig. 2), have been modelled as a time dependent temperature boundary condition, according to the measurements.

To avoid convergence problems due to non-orthogonal or skewed cells, cell limited and non-orthogonal corrected schemes are used for gradient, divergence, laplacian and surface normal gradient discretization. Using the cell limited scheme face values, extrapolated from a cell value using the calculated gradient, are limited such, that the face value does not fall out of bounds anymore. Room temperature and zero gas velocity in the whole simulation domain where used for initial conditions.

Simulations have been carried out in parallel using MPI parallelization on the Vienna Scientific Cluster (VSC3), the whole simulation domain was decomposed into up to 480 sub-domains using the simple decomposition method (OpenFOAM v4 User Guide, The OpenFOAM Foundation (Ferzinger and Peric, 2002). Depending on the total number of cells, simulation took up to 84 h to complete.

5. Design of simulation experiments

In previous studies focused on the CFD-simulation of heat transfer in packed beds, mainly particles with low thermal conductivity were used (Table 2). Moreover, mostly setups with forced fluid flow have been investigated. Here convection will dominate and conduction only plays a secondary role.

To get the optimal bridge sizes d/D and effective thermal conductivities $k_{eff,mod}$, similar approach as Design of Experiments has been used. In this approach, the design has been performed on a set of simulation instead of experiments. Therefore it is called Design of Simulation Experiments (DoSE).

In this set of experiments, a number of factors are varied and their effect on the system response (see Chapter 5.2) is studied. By using DoSE, the number of simulation runs necessary to achieve a certain goal (screening, optimization), and therefore invested time and design costs, can be reduced compared to the" intuitive" COST (Change only One Separate factor at a Time) approach (Lawson, 2015; Eriksson et al., 2008).

5.1. *DoSE factors*

The factors are the variables that, due to changes in their level, will influence the response of the system or the process. After defining the factors, their ranges need to be specified. The range might be limited by the simulation settings or objectives, as well as by physical constraints. For the DoSE in this study aluminium spheres and the following factors and levels have been used.

1 Particle size D: 6, 10 mm
2 Bridge size d/D: 0.15, 0.2
3 Multiplier k for the bridges effective thermal conductivity k_{eff}: 0.5, 1.5

$$k_{eff,mod} = k\,k_{eff} \tag{17}$$

The effective thermal conductivity k_{eff} is calculated using Eqs. 1–7.

Goal of the DoSE study was to recommend a bridge size d/D to use in heat transfer simulations. The particle size D was included as a factor to see if the bridge size needs to be changed for different particle sizes. To be able to further

Table 2 – Comparison of thermal conductivities of particles used in different studies.

Study	Material	k_p, W / (m K)	ρ_p, kg / m^3	c_p, J / (kg K)	$Re_{Particle}$, -
Dixon et al. (2013)	Alumina	1	1947	1000	500 - 10,000
Dixon et al. (2012)	Alumina	0.25	2000	1000	1600 - 5600
	Nylon	0.4	1140	1700	2200 - 27,000
Wehinger (2016)	–	5	1300	1000	35, 700
This study	Aluminium (DoSE)	236	2700	837	<1
	Steel (validation)	54	7850	430	

decrease the deviation from experiment to simulation, the correction factor k was also included in the DoSE.

5.1.1. *Response*

It is important to select a response that is relevant with respect to the problem formulation. Thus, the residual of the temperature at the centre point of the packing's top surface at a specific time, was selected as the system response. Here, the residual is defined as the difference of the simulated and the measured surface temperature. The measured temperature at t = 0 s was offset corrected to match the initial simulation temperature and is therefore referred as *corrected*. A residual of zero refers to a perfect prediction the surface temperature at a given time t. A negative or positive residuum refers to an under- or over-prediction of the surface temperature, respectively. The residuum was calculated after the packing surface temperature increased by 4.5 K, compared to the starting temperature.

$$\Delta T_{response} = T_{sim}(t) - T_{exp}(t) \tag{18}$$

at

$$\Delta T_{exp} = T_{exp}(t) - T_{exp}(t = 0) = 4.5\,K \tag{19}$$

5.2. *The design*

Depending on the objective, one may choose different designs, which represent combinations of factors and the levels used in all the simulation experiments. For screening usually fractional factorial designs are sufficient, while full factorial designs or central composite designs are needed for optimization (The OpenFOAM Foundation, 2019).

A design with three factors and two levels each (full factorial design or 2^3 FFD) was used to study the effect of the factors on the response to optimize the parameters to match experiments. The worksheet representation of the design, containing the factors, their levels and the modified effective thermal conductivities of the bridges $k_{eff,mod}$ are shown in Table 3. According to the design, four packed bed geometries were prepared for CFD simulation with particle diameters of D =6 mm (619 particles) and D = 10 mm (200 particles) and bridge diameter to particle diameter ratios of 0.15 and 0.2. For the generation and analysis of the design, the software package R (R Core Team, 2018) and the GUI RStudio (R Studio Team, 2016) were used.

5.3. *The model*

The three main types of polynomial models, which are frequently used in DoSE are linear, interaction, and quadratic models. The choice of which model to use is not completely free. If screening was selected as the objective, either a linear or an interaction model is pertinent. If optimization is the objective of the DoSE, an interaction model or a quadratic model are most suitable (The OpenFOAM Foundation, 2019).

Using a 2^3 full factorial design, it is possible to estimate interaction models. For the three factors and the chosen response described in the previous section, a possible interaction model is given by

$$\Delta T_{response} = \beta_0 + \beta_D x_D + \beta_{d/D} x_{d/D} + \beta_k x_k + \beta_{D:d/D} x_D x_{d/D} + \beta_{D:k} x_D x_k + \beta_{d/D:k} x_{d/D} x_k \tag{20}$$

Here β_i, β_{ij}, x_i, xj are the main effects coefficients, interaction coefficients and factors, respectively. For better readability the main effects coefficients, interaction coefficients are referred by their index only (e. g. $d/D : k$ instead of $\beta_{d/D:k}$) in the following sections.

5.4. *The DoSE diagnostic tools*

5.4.1. *Half-normal plot*

The half normal plot is a graphical diagnostic tool to evaluate the goodness of a Do(S)E fit. In the plot, the ordered absolute values of estimated factors are compared to the theoretical ordered statistic medians from a half-normal distribution. The half normal distribution is the distribution of |X|, where X follows a normal distribution. The absolute value of an estimated factor x_i is calculated as follows:

$$factor\ x_i\ effect = \left|\overline{Y}(+) - \overline{Y}(-)\right| \tag{21}$$

where $\overline{Y}(+)$ is the average of all responses where the factor x_i takes on a 'high' level and $\overline{Y}(-)$ is the average of all responses where the factor x_i takes on a 'low' level. In the half normal plot unimportant factors now appear near zero and on a line, while important factors appear well of zero and off the line.

5.4.2. *Response plot*

In a response plot, the systems responses are plotted over the experimental runs. For simple designs, the response plot is a viable tool to identify a qualitative influence of different factors on the response.

5.4.3. *Shapiro-Wilk Test*

The null hypothesis of this test is that the sample came from a normally distributed population. If the p-value is less than the chosen significance level (or α-level), the null hypothesis is rejected, thus the data are not likely to be normally distributed. On the other hand, if the p-value is higher than the α-level, the null hypothesis cannot be rejected. Then there is evidence that the data are normally distributed. A α-level of 5 % was used in this study.

Table 3 – Screening design for three factors and the response ΔT. $k_{eff,mod}$ according to Eq. 17.

Run	D, mm	d/D	k	$k_{eff,mod}$, W/(m K)
0	6	0.15	0.5	0.0512
1	10	0.15	0.5	0.0577
2	6	0.20	0.5	0.0588
3	10	0.20	0.5	0.0653
4	6	0.15	1.5	0.1537
5	10	0.15	1.5	0.1732
6	6	0.20	1.5	0.1763
7	10	0.20	1.5	0.1959

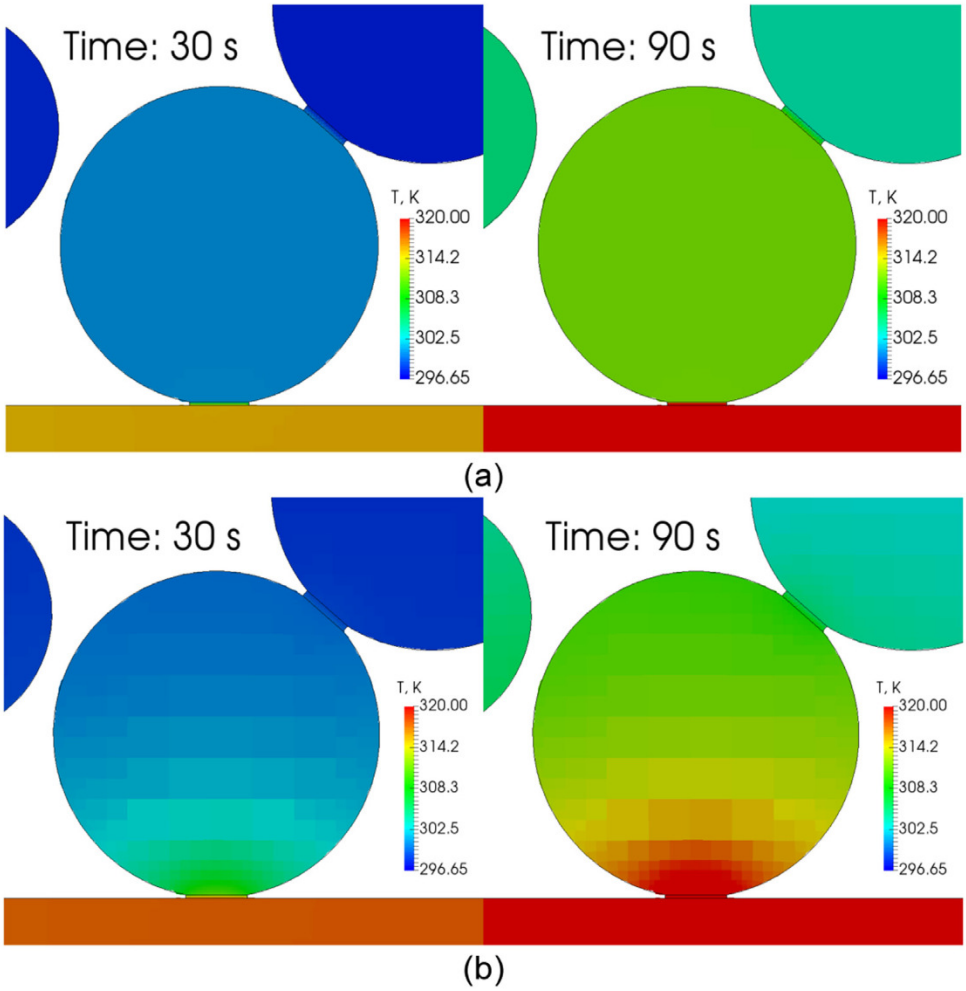

Fig. 5 – Temperature distribution in two adjacent spheres on a heated plate, in a packing consisting of spheres. (a) aluminium spheres (k_p = 236 W / (m K)), (b) low thermal conductivity (k_p = 1.1 W / (m K)).

5.5. *Influence of the thermal conductivity of the particles*

For materials with high thermal conductivity (e.g. aluminium), the conductivity of the bridges has big influence on the overall heat transfer, as the representing contact points are the main resistance (Bu et al., 2020). Therefore, small changes in the thermal conductivity of the bridges do have significant influence on the overall bed conductivity. There is nearly no temperature gradient inside the spheres for high thermal conductivities. This fact is shown in Fig. 5 (a), where the temperature distribution in two adjacent spheres after 30 and 90 simulated seconds is shown. For spheres with lower thermal conductivity ((k_p = 1.1 W / (m K)), Fig. 5b) the temperature gradient in the single spheres is much higher, which means that the share of heat transfer resistance in the bridges on the overall heat transfer resistance, is much lower compared to aluminium.

6. Results and discussion

6.1. *DoSE results*

The surface temperatures for each of the eight performed simulations and experiments and the calculated response $\Delta T_{response}$ are shown in Table 4. Experiments have been carried out up to three times with newly randomized packings. The difference in the surface temperature between experiments at a given time was within ± 0.15 K. To ensure the representativity of a single point measurement for the whole surface, the simulated surface temperature distribution is compared to images taken with the infrared-camera. In Fig. 6 good agree-

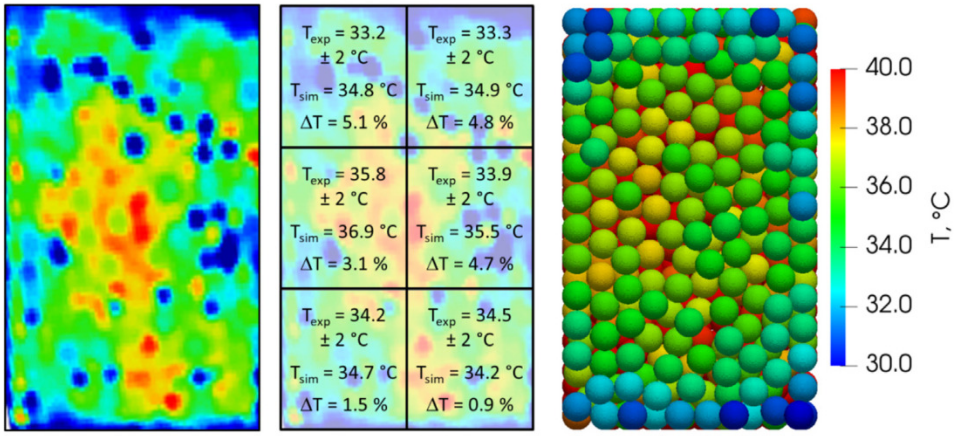

Fig. 6 – Surface temperature distribution of a packed bed consisting of 619 aluminium spheres after 10 min. (a) Experiment, (b) average surface temperatures and relative deviation in % of marked areas, (c) Simulation (Run 6).

Table 4 – Responses for performed simulations/experiments.

Run	T_{exp}, K	T_{sim}, K	$\Delta T_{response}$, K
0	301.15	299.07	−2.08
1	302.15	297.94	−3.21
2	301.15	298.76	−2.39
3	302.15	297.66	−3.49
4	301.15	301.84	0.69
5	302.15	300.7	−0.45
6	301.15	302.63	1.48
7	302.15	300.93	−0.22

ment of the experimental and simulated surface temperature of a packing consisting of 619 spheres with diameter of 6 mm (Run 6 in Table 4) can be seen. Thus, the point wise response values are considered as valid.

The contribution of conductive heat transfer to the overall heat transfer was evaluated for two spheres in the packing. One of the situated on the bottom most layer of the packing, the other one on the packings surface. The share of conductive heat flux to the spheres are 65–99 %, depending on the exact case (D, d/D, k), the position of the sphere and the evaluated time. It is concluded, that conduction is the dominant heat transfer mechanism in the packing.

Small deviation of $\Delta T_{response}$ from zero can be seen in Table 4 for k = 1.5 (run 4–7), while for k = 0.5 (run 0–3) the deviations from experiment to simulation are higher. Also 6 mm particles (runs0,2,4,6) show higher packing surface temperatures in the simulation runs than 10 mm spheres (runs1,3,5,7), for the same bridge size (d/D-ratio) and k-value. For 10 mm spheres, the simulated surface temperature is always lower than the experimental surface temperature (negative response).

To test if the response is likely to come from a normally distributed population a Shapiro-Wilk Normality test is performed. As the resulting probability-value 0.5638 for the Shapiro-Wilk test is higher than any reasonable significance level (α-level, e.g. α = 0.05), the null hypothesis cannot be rejected. Thus, $\Delta T_{response}$ is likely to come from a normally distributed population and an interaction model can be fitted to the data.

A half-normal plot (Fig. 7) reveals that only two individual factors, namely the sphere size D and the multiplier k, do have significant influence on the response (α = 0.05). Based on this,

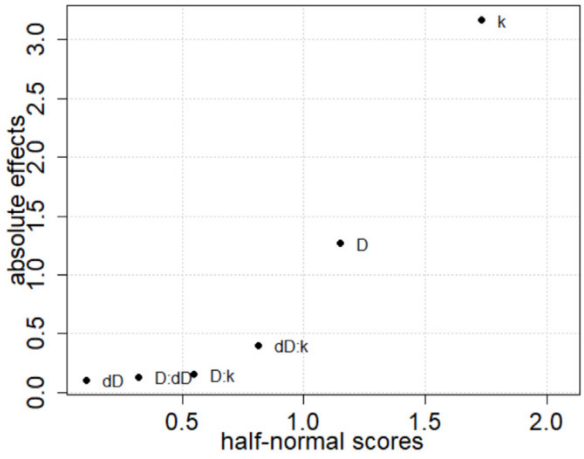

Fig. 7 – Half-normal plot for influence of parameters on the respond.

a simpler two-parameter model containing only significant parameters was fitted to the results achieving a coefficient of determination of $R^2 = 0.98$. When considering only significant factors Eq. 20 reduces to

$$\Delta T_{response} = \beta_0 + Dx_D + kx_k \tag{22}$$

The prediction error of Equation (22) for $\Delta T_{response}$ is ± 0.3 K, with the exception of Run 6. Here the prediction error is 0.47 K. Using this equation, the multiplier k for the bridges' effective thermal conductivity can now be calculated for a given sphere and bridge size by setting $\Delta T_{response}$ to zero.

$$k = 0.581 + 100\,D \tag{23}$$

Here D is the particle diameter in m. Using this equation, the effective thermal conductivity for bridges, calculated using Eq. 1 – 7, can now be corrected and optimized for different sphere diameters.

As shown in this study and in literature (e.g. Wehinger, 2016; Cheng et al., 2020). With increasing Reynolds numbers the contribution of conduction to the overall heat transfer decreases and the effective thermal conductivity of the bridges is less important (shown by e.g. Wehinger, 2016); Cheng et al., 2020). Despite this sinking share on the overall heat transfer with increasing Reynolds numbers, the conduc-

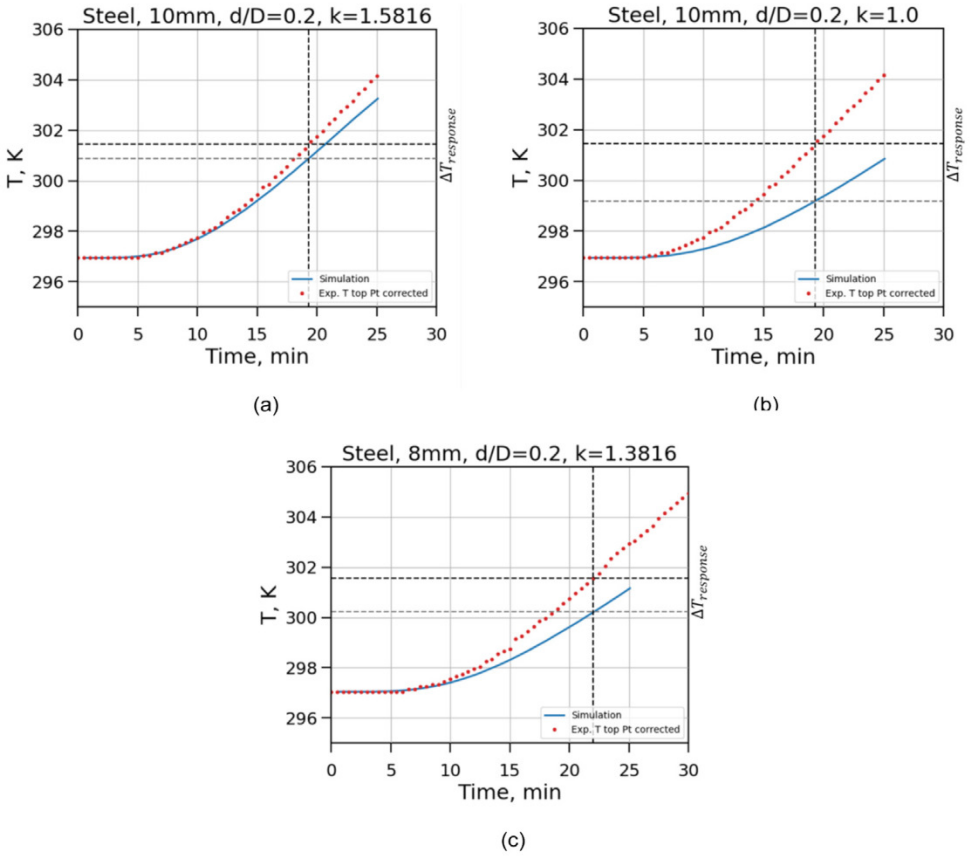

Fig. 8 – Comparison of CFD-simulation results and experimental surface temperature for steel spheres using an effective thermal conductivity using modified thermal conductivity according to Eq. 23: (a) 10 mm spheres with corrected thermal conductivity, (b) 10 mm spheres with uncorrected thermal conductivity, (c) 8 mm spheres with corrected thermal conductivity.

tion through particle-particle contact points can and should be corrected using the presented correction factor. The impact of the correction will decrease when convection becomes the dominant heat transfer mechanism. Still, the contribution of conduction to the overall heat transfer in the packed bed can be simulated with higher accuracy when considering flattening at contact points, surface roughness and non-spherical particles, by correcting the bridges thermal conductivity.

As stated before, the correction factor presented in Equation (23) can be interpreted as an indicator for flattening of particles at the contact points. As the correction factor is applied to Eqs. 1–7, where no flattening is considered, one could argue that k should be ≥ 1. Where k = 1 indicates no flattening at contact points. This results in a minimum D of 4.2 mm. Also the application of the presented model outside the studied region is not recommended.

6.2. *Generalization*

For validation and generalization of the findings of Chapter 6.1, additional experiments and simulations have been carried out for material with a different (lower) thermal conductivity (steel) and different sphere diameters.

In Fig. 8 (a), a comparison of experiment and simulation for D = 10 mm steel spheres, using bridges of the size of d/D = 0.2 and the linear model for the multiplier k for effective thermal conductivity in the bridges (Eq. 23) is shown. Here the simulation underestimates the surface temperature. The temperature difference after 19 min is −0.57 K. Compared to a case with an unmodified effective thermal conductivity (Fig. 8b, ΔT = −2.26 K) the error $\Delta T_{response}$ was reduced by 75 % (1.69 K).

The simple linear model was then used in the simulation of d =8 mm steel spheres (bed consisting of 496 spheres - Fig. 8c), where the bridge size was set to d/D = 0.2. 8 mm spheres do represent the centre point of the full factorial design from Section 6.5.3, which is covered in terms of experimental region, but not directly included in design as point. One can see that the simulated temperature is lower than in the experiments (ΔT = −1.32 K). That indicates that the linear model might not be sufficient to describe the effective thermal conductivity in this design point.

6.3. *Conclusion and outlook*

Based on the referenced studies the bridges method should give reasonable results for simulating flow and heat transfer in the packed beds with forced convection. In the present study, the impact of the bridges method on the simulated heat transfer has been studied without forced convection, reducing convective heat transfer as much as possible. A set of experiments and simulations was carefully selected using Design of Simulation Experiments. Using the bridges method and a full factorial DoSE reveals that the bridge size has a negligible influence on the heat transfer in packed beds, for the tested range of particle diameter and bridge sizes.

It was shown that the simple linear model, k = 0.581 + 100 D for correcting thermal conductivities of the bridges, can be used to give estimates for the bridges effective thermal conductivity at the tested experimental points. The error for one

example case (D = 10 mm steel spheres and a bridge size of d/D = 0.2) at a representative point of the DoSE was reduced by 75 % from 2.26 K to 0.57 K using this model compared to an unmodified effective thermal conductivity in in the bridges.

It was shown that conduction is the dominant heat transfer mechanism for the studied packings with low Reynolds numbers. Thus, the correct prediction of the bridges thermal conductivity is essential to get simulation results that are in good agreement with the experiments. Summing up, the use of the bridges method in conjunction with the presented correction factor for the simulation of packings consisting of spheres with a diameter of D = 6–10 mm is recommended.

Additional optimization designs should be performed in future works. Especially the interaction of the bridge size and the conductivity of the bridge need further investigations. Thus a wider range of bridge sizes and particle diameter should be used in optimization.

To be able to generalize the model further for the effective thermal conductivity of bridges between particles, the influence of additional parameters (such as flattening of particles or surface roughness) should be studied.

Declaration of interests

The authors declare that they have no known competing financial interests or personal relationships that could have appeared to influence the work reported in this paper.

Nomenclature

Symbol	Description	Unit
$c_{p,g}$	gas heat capacity	J/(kg K)
$c_{p,s}$	solid heat capacity	J/(kg K)
C	constant for calculation of the accommodation coefficient	-
d	bridge diameter	m
D	particle diameter	m
D_{col}	column diameter	m
h	half of the fluid conduction length	m
h_b	half the height of the bridge	m
h_i	are half of the fluid solid length	m
k	multiplier k for the bridges effective thermal conductivity	-
k_{eff}	effective thermal conductivity of bridges	W/(m K)
$k_{eff,mod}$	modified effective thermal conductivity of bridges	W/(m K)
k_f	thermal conductivity of surrounding gas	W/(m K)
k_{fr}	reduced thermal conductivity of a gas-filled gap	W/(m K)
k_p	thermal conductivity of the particles	W/(m K)
M	molar mass of the gas	kg/mol
N	bed to particle diameter ratios	-
p	pressure	Pa
Pr	Prandtl number	-
R	particle radius	m
R_{col}	column radius	m
$\mathcal{R}$	universal gas constant	J/(mol K)
r_b	bridge radius	m
Re_p	Particle Reynolds number, $\rho D_{particle} u_0/\mu$	-
r^*	reduced distance from the wall	-
t	time	s
T	temperature	K
T_{exp}	experimental temperature	K
$T_{exp\ corrected}$	experimental temperature, offset corrected	K
T_{sim}	simulated temperature	K
u	velocity	m/s
u_0	superficial velocity	m/s
x_{min}	parameter for calculation of r^*	m
z	non dimensional distance from the wall	-

Greek Letters		
α	significance level	-
β	main effects coefficients, interaction coefficients	-
Δt	time step size	s
Δx	cell size	m
$\Delta T_{response}$	DoSE response	K
γ	accommodation coefficient	-
Λ	mean free path of the gas molecules	m
μ	dynamic fluid viscosity	Pa s
ρ	density	kg/m^3
ψ	packed bed porosity	-
ψ_∞	porosity of an infinitely extended bed	-

Declaration of Competing Interest

The authors report no declarations of interest.

Acknowledgement

The computational results presented have been achieved in part using the Vienna Scientific Cluster (VSC).

This work used the software discreteFlow which is developed by B. Haddadi, H.R. Norouzi, C. Jordan and M. Harasek in cooperation with TU Wien (Austria) and Amirkabir University of Technology Tehran, Iran) with support by chemical-engineering.at and numerics GmbH.

Partial financial support was provided by the Austrian research funding association (FFG) under the scope of

the COMET program within the research project Industrial Methods for Process Analytical Chemistry From Measurement Technologies to Information Systems (imPACts, www.k-pac.at) (contract # 843546).

Part of this research was financially supported by CHASE. CHASE is a COMET Centre within the COMET – Competence Centers for Excellent Technologies Programme and funded by BMVIT, BMDW. The COMET Programme is managed by Austrian research funding association (FFG project number 868615).

References

VDI-Wärmeatlas. VDI-Wärmeatlas. s.l. : Springer-Verlag Berlin Heidelberg, 2013. Vol. 11.

Behnam, M., et al., 2013. A new approach to fixed bed radial heat transfer modeling using velocity fields from computational fluid dynamics simulations. Ind. Eng. Chem. Res. 52, 15244–15261.

Bey, Oliver, Eigenberger, Gerhart, 1997. Fluid flow through catalyst filled tubes. Chem. Eng. Sci. 52, 1365–1376.

Bu, S.S., et al., 2014. On contact point modifications for forced convective heat transfer analysis in a structured packed bed of spheres. Nucl. Eng. Des. 270, 21–33.

Bu, Shanshan, et al., 2020. Numerical and experimental study of stagnant effective thermal conductivity of a graphite pebble bed with high solid to fluid thermal conductivity ratios. Appl. Therm. Eng. 164.

Cheng, Guojian, Gan, Jieqing, Xua, Delong, Aibing, Yu, 2020. Evaluation of effective thermal conductivity in random packed bed: heat transfer through fluid voids and effect of packing structure. Powder Technol. 361, 326–336.

deKlerk, Arno, 2003. Voidage variation in packed beds at SmallColumn to particle diameter ration. AIChE J. 49, 2022–2029.

Dixon, A.G., Nijemeisland, M., 2001. CFD as a design tool for fixed-bed reactors. Ind. Eng. Chem. Res. 40, 5246–5254.

Dixon, A.G., et al., 2011. Systematic mesh development for 3D CFD simulation of fixed beds: single sphere study. Comput. Chem. Eng. 35, 1171–1185.

Dixon, A.G., et al., 2012. Experimental validation of high Reynolds number CFD simulations of heat transfer in a pilot-scale fixed bed tube. Chem. Eng. J. Vols. 200-202, 344–356.

Dixon, A.G., Nijemeisland, M., Stitt, E.H., 2013. Systematic mesh development for 3D CFD simulation of fixed beds: contact points study. Comput. Chem. Eng. 48, 135–153.

Eppinger, T., Seidler, K., Kraume, M., 2011. DEM-CFD simulations of fixed bed reactors with small tube to particle diameter ratios. Chem. Eng. J. 166, 324–331.

Ergun, Sabri, 1952. Fluid flow through packed columns. Chem. Eng. Prog. 48, 89–94.

Eriksson, L., et al., 2008. Design of Experiments; Principles and Applications, Vols. 3. Umetrics Academy.

Ferzinger, J.H., Peric, M., 3rd 2002. Computational Methods for Fluid Dynamics. Springer, Berlin.

Guardo, Alfredo, et al., 2004. CFD flow and heat transfer in nonregular packings for fixed bed equipment design. Ind. Eng. Chem. Res. 43, 7049–7056.

Kuroki, M., et al., 2007. High-fidelity CFD modeling of particle-to-fluid heat transfer in packed bed reactors. Proceedings of European Congress of Chemical Engineering (ECCE-6) 9.

Lawson, John (Ed.), 2015. Design and Analysis of Experiments With R. CRC Press, Boca Raton.

Norouzi, Hamid Reza, et al., 2016. Coupled CFD-DEM Modeling. John Wiley & Sons, Ltd.

Ookawara, S., et al., 2007. High-fidelity DEM-CFD modeling of packed bed reactors for process intensification. Proceedings of European Congress of Chemical Engineering (ECCE-6) 9.

R Core Team, 2018. R: A Language and Environment for Statistical Computing. Vienna https://www.R-project.org/.

R Studio Team, 2016. RStudio: Integrated Development Environment for R. RStudio, Inc., Boston, MA.

Shafeeyan, Mohammad Saleh, Daud, Wan Mohd Ashri Wan, Shamiri, Ahmad, 2014. A review of mathematical modeling of fixed-bed columns for carbon dioxide adsorption. Chem. Eng. Res. Des. 92, 961–988.

The OpenFOAM Foundation, 2019. OpenFOAM v4 User Guide, visited on 2019-09-08 https://cfd.direct/openfoam/user-guide/.

Wehinger, Gregor Dionys, 2016. Particle-resolved CFD Simulations of Catalytic Flow Reactors. Technischen Universität Berlin.

Yang, Jian, et al., 2012. Experimental analysis of forced convective heat transfer in novel structured packed beds of particles. Chem. Eng. Sci. 71, 126–137.